Sensors & Diagnostics

PAPER

View Article Online
View Journal | View Issue

Check for updates

Cite this: *Sens. Diagn.*, 2025, **4**, 166

Construction of a self-assembled duplexed aptasensor for the simultaneous detection of haemoglobin and glycated haemoglobin†

Xue-Qing Feng,[ab] Yi-Ning Su,[a] Qing Li,[b] Zhong-Gan Jin,[b] Ming Wang,[b] Xi-Le Hu,*[a] Lei Zou,*[a] Yi Ju,*[bc] Xiao-Peng He *[ad] and Bang-Ce Ye *[c]

Received 11th September 2024,
Accepted 13th December 2024

DOI: 10.1039/d4sd00303a

rsc.li/sensors

With the prevalence of diabetes and its secondary complications, the effective monitoring of diabetic biomarkers is necessary. While portable analytical devices for blood glucose have been sophisticatedly developed, those for haemoglobin (Hb) and, especially haemoglobin A1c (HbA_{1c}), a glycated form of Hb, remain elusive. Here, we developed an aptamer-based duplexed electrochemical sensor for the simultaneous detection of Hb and HbA_{1c}. Ferrocene (Fc) and a thiol group were introduced to the 5′ and 3′-end of aptamers that bind Hb and HbA_{1c}, respectively. While the thiol group facilitates the formation of a self-assembled monolayer of the aptamers onto a customized, duplexed screen-printed gold electrode, the presence of Fc provides the electrodes an internal electrochemical signal. Upon analyte binding, the secondary conformation of the aptamers is changed, thus leading to a quenched current signal because of an increased distance between Fc and the electrode surface. Our duplexed electrochemical sensor showed a good linearity for both analytes over a wide concentration range, and has proved effective in simultaneously quantifying Hb and HbA_{1c} in calibration samples.

Open Access Article. Published on 10 ianuarie 2025. Downloaded on 19.04.2026 01:31:34.
This article is licensed under a Creative Commons Attribution 3.0 Unported Licence.

Introduction

According to The International Diabetes Federation (IDF), in 2023, there were 537 million people diagnosed with diabetes worldwide (10% of the world's adult population).[1] The diagnosis, monitoring and treatment of diabetes cost ~548 billion US dollars per year, which accounts for 11% of the world's total health-care costs.[2] By 2045, the number of people with diabetes worldwide is estimated to reach 783 million. According to a report by the Chinese Diabetes Society (CDS), the predicted number of diabetic patients in China reached 141 million (aged 20–79) in 2021, of which 51.7% were undiagnosed and 1.4 million died. According to the International Diabetes Federation, an estimated diabetes-related expenditure was 165.3 billion USD in 2021, which poses a large social and economic burden on the world health-care system.[3]

While the monitoring of blood glucose offers guidance for risks of diabetes, the detection of haemoglobin (Hb) in its glycated form is the gold standard for the definite diagnosis of diabetes. Clinically, chromatographic techniques are employed to quantify Hb and HbA_{1c} (a glycated form of Hb) in the whole blood, and the HbA_{1c}/Hb ratio is used as a measure for diagnosing diabetes. This method is time-consuming and requires complicated sample pre-treatment, and therefore is not suitable for point-of-care testing (POCT). The use of antibodies to directly capture Hbs is an alternative to chromatographic approaches. Antibodies are generally labelled with a colorimetric, fluorescent or chemiluminescent (CL) species for immunosorbent assays.[4] This method facilitates the POCT of Hbs to be achieved in the form of paper strips (with colorimetric and fluorescent labels) and miniature bedside facilities (with CL labels). However, antibodies face challenges in terms of shelf-stability, reproducibility from batch to batch and interference from autoantibodies and heterophil antibodies existing in the human blood. Attempts of using phenylboronic acid derivatives to bind glycated Hbs have also been made,[5–7] but the propensity of boronates to unselectively binding diols that

[a] *Key Laboratory for Advanced Materials and Joint International Research Laboratory of Precision Chemistry and Molecular Engineering, Feringa Nobel Prize Scientist Joint Research Center, School of Chemistry and Molecular Engineering, East China University of Science and Technology, 130 Meilong Rd., Shanghai 200237, China. E-mail: xlhu@ecust.edu.cn, zoulei@ecust.edu.cn, xphe@ecust.edu.cn*

[b] *Shanghai Center for Clinical Laboratory, 528 Hongshan Road, Pudong, Shanghai, 200126, P.R. China. E-mail: juyi@sccl.org.cn*

[c] *Laboratory of Biosystem and Microanalysis, State Key Laboratory of Bioreactor Engineering, East China University of Science and Technology, Shanghai 200237, China. E-mail: bcye@ecust.edu.cn*

[d] *National Center for Liver Cancer, The International Cooperation Laboratory on Signal Transduction, Eastern Hepatobiliary Surgery Hospital, Shanghai 200438, China*

† Electronic supplementary information (ESI) available. See DOI: https://doi.org/10.1039/d4sd00303a

© 2025 The Author(s). Published by the Royal Society of Chemistry

Open Access Article. Published on 10 ianuarie 2025. Downloaded on 19.04.2026 01:31:34.
This article is licensed under a Creative Commons Attribution 3.0 Unported Licence.

are structurally diverse in humans might compromise the accuracy of this approach.

Electrochemical sensors have been extensively developed for biosensing. By using portable electrochemical workstations and miniaturized screen-printed electrodes (SPEs), the POCT of a variety of disease-relevant biomarkers has been achieved.[8] Both self-assembly and covalent conjugation could be used to functionalize working electrodes with a capture agent (antibodies, peptides, aptamers, carbohydrates, *etc.*) to selectively bind an analyte of interest. The capture of the analyte subsequently causes a signal variation through perturbing the redox kinetics of the electrochemical system. With this sensing rationale, electrochemical sensors based on diffused (such as $Fe(CN)_6^{3-}/Fe(CN)_6^{4-}$, $Ru(NH_3)_6^{3+}$ and Hemin/G4) and embedded electroactive species (such as ferrocene (Fc), methylene blue (MB) and anthraquinone (AQ)) have been successfully constructed.[9–12] However, electroactive sensors for the simultaneous detection of Hb and HbA_{1c} are elusive.

Here, we developed a duplexed aptamer-based electrochemical sensor (aptasensor) for the simultaneous detection of Hb and HbA_{1c} (Fig. 1). Aptamers are short DNA or RNA sequences with a defined secondary structure to selectively bind ions, small molecules and biomacromolecules.[13–16] Because of their relatively small size, simplicity in functionalization with other molecules, low immunogenicity, minimal batch-to-batch variation and physical stability, aptamers have been extensively used for biosensing and targeted delivery of imaging and therapeutic agents.[17–19] In this study, Fc and a thiol group were introduced to the 5′- and 3′-end of previously reported aptamers for Hb and HbA_{1c}, respectively. An SPE with dual gold working electrodes whose redox signals could be measured in a duplexed manner was customized. One electrode was modified with the Hb aptamer and the other with HbA_{1c} aptamer, both through thiol-gold self-assembly. Moreover, mercaptoethanol (MEH) was used as a blocking agent to reduce non-specific adsorption.[20] Using a portable electrochemical workstation, our experimental results demonstrated the effectiveness of the electrode system for the simultaneous sensing of Hb and HbA_{1c} and the quantification of their concentrations in calibration samples.

Results and discussion

Two aptamers, **apHb** and **apHbA$_{1c}$**, which are reported to selectively bind Hb and HbA_{1c} were synthesized according to a previous report, respectively (Fig. 1).[21] To the 5′ and 3′-end of the aptamers, the electroactive Fc and a thiol group were introduced, respectively. When bound to gold electrodes through thiol-gold self-assembly, an internal current signal could be measured due to the spatial proximity of Fc to the electrode surface, and upon protein binding, the conformation of the aptamers is changed, leading to a quenched current signal because of an increased distance between Fc and the electrode.

An SPE with two parallel gold working electrodes, whose electrochemical activities could be measured simultaneously on a portable workstation, was customized. The Fc-functionalized **apHbA$_{1C}$** and **apHb** aptamers were self-assembled onto the two electrodes, producing **Aptasensor 1** and **Aptasensor 2**, respectively. The gold electrodes functionalized with Fc-modified **apHbA$_{1C}$** aptamers were characterized by X-ray photoelectron spectroscopy (XPS). Binding energy values of 86.3 eV, 706.8 eV and 162.3 eV, characteristic of Au 4f, Fe 2p and S 2p, were observed (Fig. S1a and b†), respectively, indicating the successful assembly of the aptamers onto the electrodes. Cyclic voltammetry (CV) was used to characterize the electroactivity of the aptamer-assembled electrodes. By applying an increasing sweep speed of 0.02–0.2 V s^{-1}, typical cyclic voltammograms of **Aptasensor 1** (Fig. 2a) and **2**-functionalized (Fig. 2b) electrodes

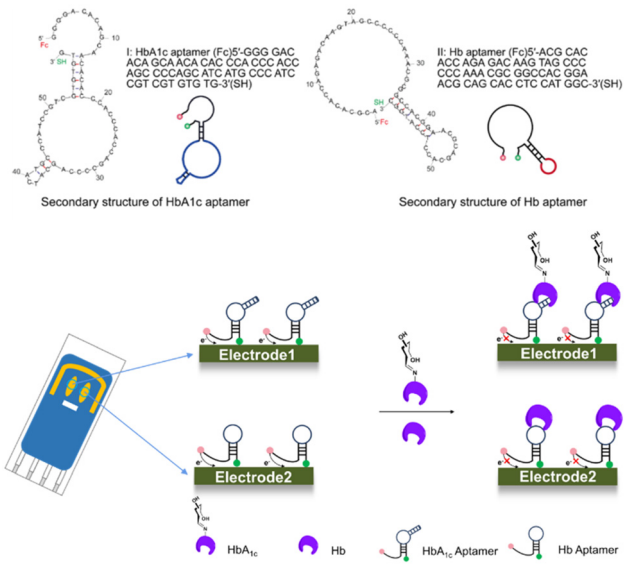

Fig. 1 Predicted secondary structure of the aptamers used in this study, and a scheme illustrating the sensing mechanism of the ferrocene (Fc)-labelled aptasensor for Hb and HbA_{1c}.

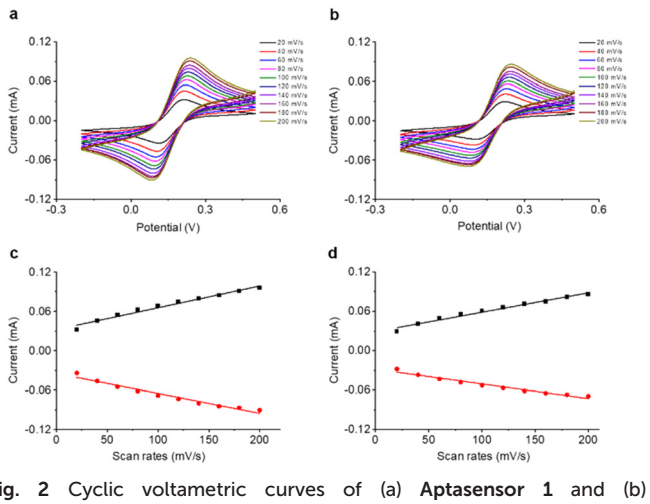

Fig. 2 Cyclic voltametric curves of (a) **Aptasensor 1** and (b) **Aptasensor 2** as a function of potential (−0.2–0.6 V). Plotting the current intensity of (c) **Aptasensor 1** and (d) **Aptasensor 2** with different scan rates (20–200 mV s^{-1}).

Open Access Article. Published on 10 ianuarie 2025. Downloaded on 19.04.2026 01:31:34.
This article is licensed under a Creative Commons Attribution 3.0 Unported Licence.

over a scanning range of −0.2–0.6 V were obtained. An electrolytic reduction and oxidation peak at 0.22 V and 0.13 V, characteristic of potassium ferricyanide, were observed for both electrodes, respectively. Plotting the current intensity of **Aptasensor 1** (Fig. 2c) and **2**-functionalized (Fig. 2d) electrodes as a function of potential produced good linearity for both the oxidation and reduction peak. In addition, we found that the current of the aptasensors at both peaks scaled up linearly as the scan rate increases, suggesting the redox process was surface-controlled.[22] A surface coverage amount (Γ^*) of **apHb** and **apHbA$_{1c}$** was calculated to be 2.19×10^{-11} M cm^{-2} and 1.92×10^{-11} M cm^{-2}, respectively. The results obtained from CV demonstrated the successful self-assembly of the Fc-modified aptamers onto the gold electrodes.

Next, electrochemical impedance spectroscopy (EIS) was used to test the aptamer–protein binding using the $Fe_3(CN)_6$/$Fe_4(CN)_6$ redox pair as the electrochemical probe (Fig. 3). In their representative Nyquist plots, we found a concentration-dependent increase in the capacitive resistance of both **Aptasensor 1** (Fig. 3a) and **2** (Fig. 3b) in the presence of increasing concentrations of Hb and HbA$_{1c}$, respectively. In addition, an equivalent circuit was used to fit the Nyquist plots (Fig. S2†), and parameters of charge transfer resistance (R_{ct}) were obtained accordingly (Table S1†). This agrees with previous reports that the binding of an analyte to a functionalized electrode results in a larger polarization resistance being obtained.[23–25]

We also used differential pulse voltammetry (DPV) to corroborate Hb sensing (Fig. 4). The optimal detection conditions were obtained by running the tests at different scan rates (Fig. S3a and b†) and pH (Fig. S3c and d†). Similarly, we observed a gradual current drop when increasing the concentrations of Hb and HbA$_{1c}$ that were incubated with **Aptasensor 1** (Fig. 4a and c) and **Aptasensor 2** (Fig. 4b and d), respectively. This corroborates the binding of the protein to the aptamer-functionalized electrodes leading to a quenched Fc signal. We determined a dissociation constant (K_d) of 25.2 ± 6.5 μg mL^{-1} and 9.3 ± 2.0 μg mL^{-1} for Hb and HbA$_{1c}$, respectively. A linear range of 5–200 μg mL^{-1} and 0.1–24 μg mL^{-1} was determined for the detection of Hb and HbA$_{1c}$, respectively. In addition, over a clinically-relevant range of the concentration ratio between HbA$_{1c}$ and Hb (HbA$_{1c}$/Hb) (NGSP% (National Glycohemoglobin Standardization Program): 4.4–17.4%),[26,27] a good correlation was obtained for the current intensity ratio of **Aptasensor 1**/**Aptasensor 2** (Fig. S4†). These data suggest that the detection range of **Aptasensor 1** and **2** meets the requirements of clinical application. In addition, nanogram-range limit of detection was obtained for **Aptasensor 1** (49.0 ng mL^{-1}) and **2** (19.1 ng mL^{-1}). The results obtained from DPV suggest the good sensitivity of the aptasensor developed for Hb sensing. The selectivity of **Aptasensor 1** and **2** was also tested with a range of proteins and disease biomarkers including human serum albumin (HSA), immunoglobulin G (IgG), carbohydrate antigen 19-9 (CA19-9), and cancer antigen 125 (CA125) (Fig. 5 and S5†). These proteins did not cause the electrochemical signal of aptasensors to change. In addition, potential interfering species including triglyceride (TG) and

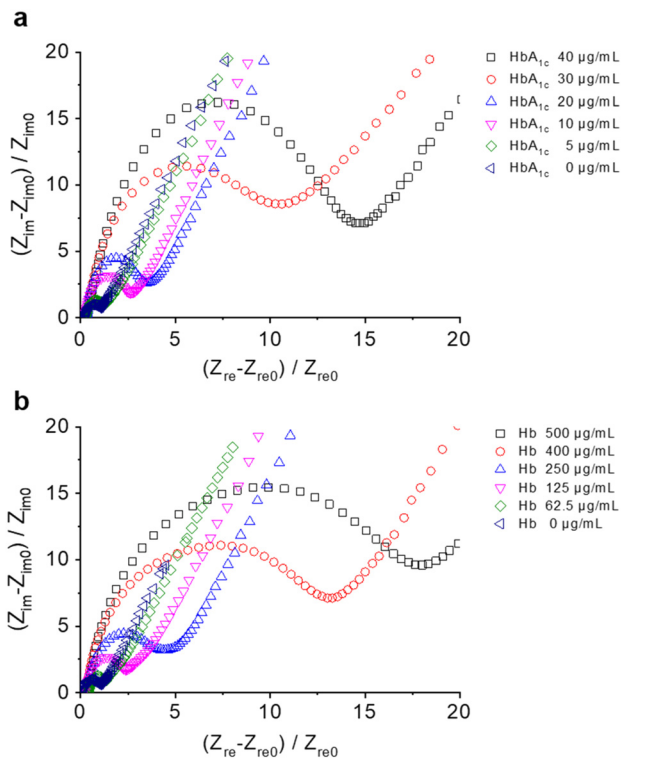

Fig. 3 Impedimetric changes of (a) **Aptasensor 1** with increasing concentrations of HbA$_{1c}$ (0–40 μg mL^{-1}) and (b) **Aptasensor 2** with increasing concentrations of Hb (0–500 μg mL^{-1}), where Z_{im} and Z_{im0} are the imaginary part of the impedimetric plots of an aptasensor in the presence and absence of HbA$_{1c}$ and Hb, and Z_{re} and Z_{re0} are the real part of the impedimetric plots of an aptasensor in the presence and absence of HbA$_{1c}$ and Hb, respectively.

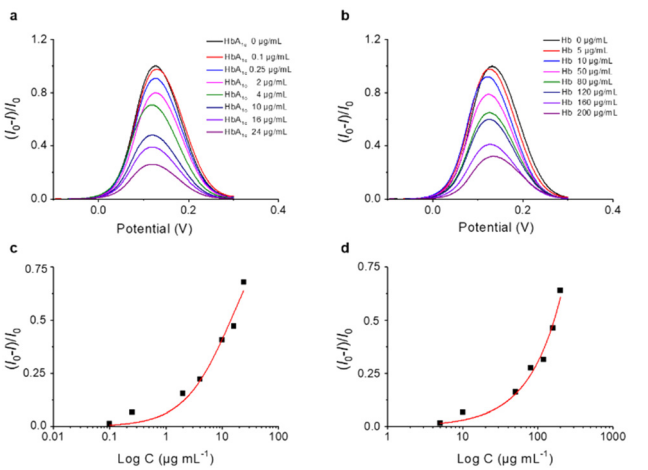

Fig. 4 Differential pulse voltammetric curves of (a) **Aptasensor 1** with increasing concentrations of HbA$_{1c}$ (0–24 μg mL^{-1}) and (b) **Aptasensor 2** with increasing concentrations of Hb (0–200 μg mL^{-1}). Plotting the current changes of (c) **Aptasensor 1** with increasing HbA$_{1c}$ (0–24 μg mL^{-1}) and (d) **Aptasensor 2** with increasing Hb (0–200 μg mL^{-1}), where I and I_0 are the current intensity of an aptasensor in the presence and absence of HbA$_{1c}$ and Hb, respectively.

© 2025 The Author(s). Published by the Royal Society of Chemistry

Open Access Article. Published on 10 ianuarie 2025. Downloaded on 19.04.2026 01:31:34.
This article is licensed under a Creative Commons Attribution 3.0 Unported Licence.

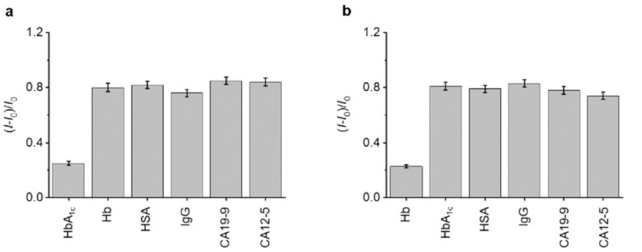

Fig. 5 Current intensity changes of (a) **Aptasensor 1** and (b) **Aptasensor 2** in the presence of selective and unselective serum proteins including hemoglobin A1c (HbA_{1c}, 50 μg mL^{-1}), hemoglobin (Hb, 50 μg mL^{-1}), serum albumin (HSA, 50 μg mL^{-1}), immunoglobulin G (IgG, 50 μg mL^{-1}), carbohydrate antigen 19-9 (CA19-9, 50 μg mL^{-1}) and cancer antigen 125 (CA125, 50 μg mL^{-1}), where I and I_0 are the current intensity of the aptasensors in the presence and absence of a protein analyte, respectively.

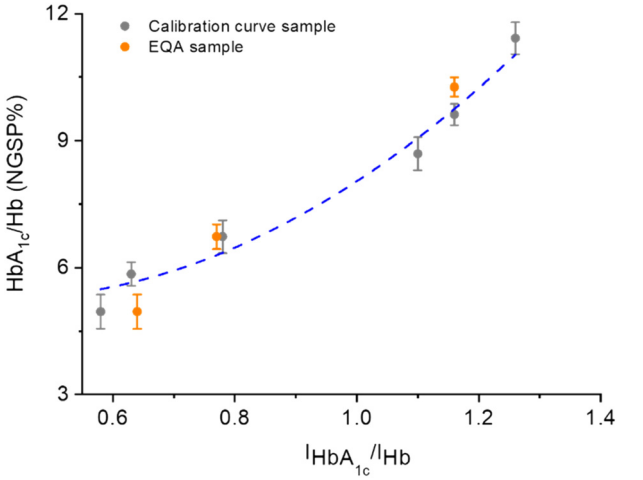

Fig. 6 Current intensity ratio changes of both **Aptasensor 1** and **2** as a function of increasing HbA_{1c}/Hb protein concentration ratios (4.96–11.42%), where I_{HbA1c} and I_{Hb} are the current intensity of **Aptasensor 1** and **Aptasensor 2**, respectively. The gray dots are the concentration points of the calibration curve samples, and the orange dots those of the external quality assessment samples.

bilirubin (BIL) were used to validate the specificity of the aptasensor (Fig. S6†), and its reproducibility was also demonstrated by measuring the same batch of HbA_{1c} (Fig. S7a and c†) and Hb (Fig. S7b and d†) samples every two days.

Finally, we sought the application of the aptasensors for the simultaneous detection of Hb and HbA_{1c} in human whole blood samples. International Federation of Clinical Chemistry and Laboratory Medicine (IFCC) certified whole-blood calibration samples were used to verify the sensing accuracy of the aptasensors. According to a standard precision and accuracy verification protocol,[28] a total of nine whole-blood calibration samples were selected, of which six (from one batch) were used to obtain a standard calibration curve, and three (from another batch) were used as external quality assessment (EQA) samples (Table S2†).

To improve the analytical accuracy, a separation material based on magnetic beads (Fe_3O_4/Au core/shell (~200 nm/20 nm) particles) to isolate Hbs prior to analysis was prepared. The beads were functionalized with the **apHb** aptamer (Fc modification at the 5′-end) through sulfhydryl-gold self-assembly.[29–32] Beads were incubated with the samples for 30 min, and then Hbs bound to the surface of the beads as a result of DNA–protein interaction were magnetically separated. Then, the bound proteins were separated using a desorption solution containing 50 mM Tris–HCl (pH 8.0) and 10 mM ethylenediamine tetraacetic acid disodium salt (EDTA) prior to detection.[33] The resulting mixtures were dripped onto the two working electrodes, and then DPV was used for the duplexed sensing to obtain the HbA_{1c}/Hb ratios of all samples. As shown in Fig. 6, a good correlation between the three EQA samples (orange dots) and the calibration curve produced from the other six samples (gray dots) was obtained. Notably, the deviation of the EQA sample with a NGSP% of 6.73% (which is close to the clinical cutoff value of NGSP% (6.5%) for diagnosis of diabetes) from the standard curve was determined to be −6.7%, which is smaller than the allowable error range (±7%) regulated by the National Center for Clinical Laboratories of China. This suggests the reliability of the aptasensor developed. A thorough comparison with previously developed sensors for HbA_{1c} and Hb detection suggests that our aptasensors are advantageous in terms of the ability to simultaneously detect HbA_{1c} and Hb; the detection range also meets the clinical detection requirements (4.96–10.27%) (Table S3†).

Conclusions

We have constructed a duplexed aptasensor for the simultaneous detection of Hb and HbA_{1c}. Aptamers modified with Fc and a thiol group were synthesized to self-assemble onto gold-based working electrodes. The surface-bound Fc gave rise to an internal current signal, which enabled the sensitive and selective detection of Hb and HbA_{1c} parallelly. Importantly, we demonstrated the real-world applicability of the aptasensor in terms of the determination of the HbA_{1c}/Hb ratio with calibration samples. We thus believe that owing to the simplicity of the sensing method and the portability of miniaturized electrochemical workstations, our proposed technique would find application in the context of POCT of Hbs.

Data availability

All key data supporting the conclusions made in this paper have been included either in the main text or in the ESI.†

Conflicts of interest

There are no conflicts to declare.

Acknowledgements

The authors thank the Natural National Science Foundation of China (NSFC) (No. 92253306, 82130099, 22477030 and 22108077),

Open Access Article. Published on 10 ianuarie 2025. Downloaded on 19.04.2026 01:31:34.
This article is licensed under a Creative Commons Attribution 3.0 Unported Licence.

the Shanghai Municipal Science and Technology Major Project (No. 2018SHZDZX03), the International Cooperation Program of Shanghai Science and Technology (No.23490711600), the Fundamental Research Funds for the Central Universities (222201717003), the Programme of Introducing Talents of Discipline to Universities (B16017), the Open Funding Project of the State Key Laboratory of Bioreactor Engineering, State Key Laboratory of Drug Research (SKLDR-2023-KF-10), and State Key Laboratory of Chemo/Biosensing and Chemometrics, Hunan University, Changsha 410082, P. R. China, and the Ministry of Education Key Laboratory on signaling Regulation and Targeting Therapy of Liver Cancer (Naval Medical University) (Grant. 2023-MEKLLC-MS/ZD-00*) for financial support. The Research Center of Analysis and Test of East China University of Science and Technology was gratefully acknowledged for assistance in analytical experiments.

Notes and references

1 E. W. Gregg, J. Buckley, M. K. Ali, J. Davies, D. Flood, R. Mehta, B. Griffiths, L. Lim, J. Manne-Goehler, J. Pearson-Stuttard, N. Tandon, G. Roglic, S. Slama and J. E. Shaw, in collaboration with the Global Health and Population Project on Access to Care for Cardiometabolic Diseases, *Lancet*, 2023, **401**, 1302–1312.
2 H. Sun, P. Saeedi, S. Karuranga, M. Pinkepank, K. Ogurtsova, B. B. Duncan, C. Stein, A. Basit, J. C. N. Chan, J. C. Mbanya, M. E. Pavkov, A. Ramachandaran, S. H. Wild, S. James, W. H. Herman, P. Zhang, C. Bommer, S. Kuo, E. J. Boyko and D. J. Magliano, *Diabetes Res. Clin. Pract.*, 2022, **183**, 109119.
3 International Diabetes Federation, *IDF Diabetes Atlas*, International Diabetes Federation, Brussels, Belgium, 10th edn, 2021.
4 J. T. Yan, S. Y. Lee, A. F. Zhang and J. Y. Yoon, *Chem. Soc. Rev.*, 2018, **47**, 6900–6916.
5 G. Murtaza, A. S. Rizvi, M. Irfan, L. S. Li and F. Qu, *J. Chromatogr. A*, 2021, **1636**, 461793.
6 P. Lakhera, V. Chaudhary, S. Singh, N. Vishwakarma, C. S. Huertas, P. Kumar and S. Kumar, *ACS Appl. Nano Mater.*, 2023, **6**, 22857–22864.
7 H. Lin and J. Yi, *Sensors*, 2017, **17**, 1798.
8 C. H. Lai, C. L. Lee, C. A. Vu, V. T. Vu, Y. H. Tsai, W. Y. Chen and C. M. Cheng, *Front. Bioeng. Biotechnol.*, 2022, **10**, 836082.
9 D. H. Xie, X. Q. Feng, X. L. Hu, L. Liu, Z. H. Ye, J. Cao, G. R. Chen, X. P. He and Y. T. Long, *ACS Appl. Mater. Interfaces*, 2016, **8**, 25137–25141.
10 M. Wahiba, X. Q. Feng, Y. Zang, T. D. James, J. Li, G. R. Chen and X. P. He, *Chem. Commun.*, 2016, **52**, 11689–11692.
11 X. P. He, B. W. Zhu, Y. Zang, J. Li, G. R. Chen, H. Tian and Y. T. Long, *Chem. Sci.*, 2015, **6**, 1996–2001.
12 X. Q. Feng, Y. Ju, W. T. Dou, Q. Li, Z. G. Jin, X. P. He, T. D. James and B. C. Ye, *Molecules*, 2021, **26**, 7077.
13 V. V. Sinitsyna and A. A. Vetcher, *Biomedicines*, 2022, **10**, 1079.
14 Y. Zhang, B. S. Lai and M. Juhas, *Molecules*, 2019, **24**, 941.
15 A. Affinito, C. Quintavalle, C. L. Esposito, G. Roscigno, C. Vilardo, S. Nuzzo, L. Ricci-Vitiani, G. D. Luca, R. Pallini, A. S. Kichkailo, I. N. Lapin, V. D. Franciscis and G. Condorelli, *Mol. Ther. Nucleic Acids*, 2019, **18**, 99–109.
16 P. K. Kulabhusan, B. Hussain and M. Yüce, *Pharmaceutics*, 2020, **12**, 646.
17 P. Röthlisberger and M. Hollenstein, *Adv. Drug Delivery Rev.*, 2018, **134**, 3–21.
18 J. C. Yan, T. Gao, Z. Z. Lu, J. B. Yin, Y. Zhang and R. J. Pei, *ACS Appl. Mater. Interfaces*, 2021, **13**, 27749–27773.
19 S. Ranallo, A. Porchetta and F. Ricci, *Anal. Chem.*, 2019, **91**, 44–59.
20 X. M. Sun, G. Z. Son, Z. J. Hu, W. J. Zhang, N. Luo and H. J. Gao, *J. Invertebr. Pathol.*, 2024, **204**, 108080.
21 H. I. Lina, C. C. Wu, C. H. Yang, K. W. Chang, G. B. Lee and S. C. Shiesh, *Lab Chip*, 2015, **15**, 486–494.
22 X. P. He, X. W. Wang, X. P. Jin, H. Zhou, X. X. Shi, G. R. Chen and Y. T. Long, *J. Am. Chem. Soc.*, 2011, **133**, 3649–3657.
23 V. Vivier and M. E. Orazem, *Chem. Rev.*, 2022, **122**, 11131–11168.
24 M. Gao and M. E. Orazem, *Electrochim. Acta*, 2021, **382**, 138226.
25 L. Bouffier, S. Arbault, A. Kuhn and N. Sojic, *Anal. Bioanal. Chem.*, 2016, **408**, 7003–7011.
26 C. D. Saudek and J. C. Brick, *J. Diabetes Sci. Technol.*, 2009, **3**, 629–634.
27 W. P. Jia, J. P. Weng, D. L. Zhu, L. N. Ji, J. M. Lu, Z. G. Zhou, D. J. Zou, L. X. Guo, Q. H. Ji, L. Chen, L. M. Chen, J. T. Dou, X. H. Guo, H. Y. Kuang, L. Li, Q. F. Li, X. Y. Li, J. Liu, X. W. Ran, L. X. Shi, G. Y. Song, X. H. Xiao, L. Y. Yang and Z. H. Zhao, *Diabetes/Metab. Res. Rev.*, 2019, **35**, e3158.
28 Q. X. Zhang, K. Bai, X. Jin, M. Zhan, L. Q. Han, J. H. Zhuang and X. Z. Huang, *J. Pharm. Biomed. Anal.*, 2024, **250**, 116396.
29 W. S. Zhao, D. X. Zhang, T. X. Zhou, J. Huang, Y. Y. Wang, B. X. Li, L. Chen, J. H. Yang and Y. Liu, *Sens. Actuators, B*, 2022, **350**, 130879.
30 Y. R. Xue, X. Li, H. B. Li and W. K. Zhang, *Nat. Commun.*, 2014, **5**, 4348.
31 S. H. Ding, Z. P. Gu, R. H. Yan, Y. G. Tang and P. Miao, *Anal. Chim. Acta*, 2018, **1029**, 24–29.
32 R. Miranda-Castro, R. Sánchez-Salcedo, B. Suárez-Álvarez, N. de-los-Santos-Álvarez, A. J. Miranda-Ordieres and M. J. Lobo-Castañón, *Biosens. Bioelectron.*, 2017, **92**, 162–170.
33 C. Forier, E. Boschetti, M. Ouhammouch, A. Cibiel, F. Ducongé, M. Nogré, M. Tellier, D. Bataille, N. Bihoreau, P. Santambien, S. Chtourou and G. Perret, *J. Chromatogr. A*, 2017, **1489**, 39–50.

© 2025 The Author(s). Published by the Royal Society of Chemistry